Journal of Power Sources 271 (2014) 589–596

Contents lists available at ScienceDirect

Journal of Power Sources

journal homepage: www.elsevier.com/locate/jpowsour

A monolithic functional film of nanotubes/cellulose/ionic liquid for high performance supercapacitors

Lucia Basiricò [a], Giulia Lanzara [a, b, *]

[a] Carbon Nanotechnology Division, Institute of Advanced Technologies (ITA), Italy
[b] Department of Engineering, University of Rome, RomaTre, Italy

HIGHLIGHTS

- Cellulose solution in CNT-based electrodes turns into a monolithic functional film.
- The monolithic nature strongly improves supercapacitors equivalent series resistance and knee frequency.
- The fabrication is significantly simpler than that of known cellulose supercapacitors.
- Superior maximum power density than CNT and non-aqueous electrolyte supercapacitors.
- The film is excellent for light-weight, flexible and pre-fabricated supercapacitors.

ARTICLE INFO

Article history:
Received 12 December 2013
Received in revised form
3 August 2014
Accepted 11 August 2014
Available online 20 August 2014

Keywords:
Supercapacitors
Vertically aligned carbon nanotubes
High power
Ionic liquid
Cellulose
Functional flexible film

ABSTRACT

A novel monolithic, pre-fabricated, fully functional film made of a nanostructured free-standing layer is presented for a new and competitive class of easy-to-assemble flexible supercapacitors whose design is in-between the all solid state and the traditional liquid electrolyte. The film is made of two vertically aligned multi-walled carbon nanotube (VANT) electrodes that store ions, embedded-in, and monolithically interspaced by a solution of microcrystalline cellulose in a room temperature ionic liquid (RTIL) electrolyte (1-ethyl-3-methylimidazolium acetate-EMIM Ac). The fine tuning of VANTs length and electrolyte/cellulose amount leads, in a sole and continuous block, to ions storage and physical separation between the electrodes without the need of the additional separator layer that is typically used in supercapacitors. Thus, physical discontinuities that can induce disturbances to ions mobility, are fully eliminated significantly reducing the equivalent series resistance and increasing the knee frequency, hence outclassing the best supercapacitors based on VANTs and non-aqueous electrolytes. The excellent electrochemical response can also be addressed to the chosen electrolyte that, not only has the advantage of leading to a significantly simpler and more affordable fabrication procedure, but has higher ionic conductivity, lower viscosity and higher ions mobility than other electrolytes capable of dissolving cellulose.

© 2014 Elsevier B.V. All rights reserved.

1. Introduction

A large spectrum of applications, such as hybrid electric vehicles, laptops, medical electronics, portable defibrillators, unmanned aerial vehicles (UAVs) and missile systems, would certainly benefit from the use of pre-fabricated and free-standing functional films that, once connected to current collectors, could be used for easy-to-assemble, environmentally friendly, safe, light-weight and flexible energy storage devices such as supercapacitors [1–4]. Standard film-based supercapacitors are typically made by assembling two electrodes and a separator impregnated with electrolyte, all sandwiched between two current collectors. While the electrodes and the electrolyte are essential functional components to let the assembly be a storage system, the separator is a passive component that is used only to avoid electrical contact between the electrodes. As of today this component has always been part of the system despite the fact that it causes a serious decrease in the supercapacitor performance during its in-service life. As discussed below, the performance reduction is mostly caused by disturbances to ions mobility generated by the undesired initiation/propagation of interfacial debond between the stacked

* Corresponding author. Carbon Nanotechnology Division, Institute of Advanced Technologies (ITA), Italy. Tel.: +39 (0)657333651.
E-mail addresses: giulia.lanzara@uniroma3.it, lanzaragiulia@gmail.com (G. Lanzara).

http://dx.doi.org/10.1016/j.jpowsour.2014.08.040
0378-7753/© 2014 Elsevier B.V. All rights reserved.

layers. In order to have the best electrochemical response, ions in the electrolyte should in fact theoretically be capable of moving freely without impacting *in* any discontinuity while traveling towards the electrodes. The interfacial problems that occur in a stacked system could be solved by making all the key components in the form of a single monolithic layer. Such an approach could lead to the realization of a pre-fabricated functional film which would be characterized by the above mentioned ideal properties (easy-to-assemble, environmentally friendly, safe, light-weight and flexible). In particular the film should be engineered in such a way to host inter-spaced and flexible electrodes impregnated with electrolyte. Simultaneously, the electrolyte, the film, the electrodes and their arrangement should be such to maximize the overall electrochemical response. This is indeed a very complex problem since it requires the optimization of several different components, materials, physical/chemical properties and phenomena. For instance, the electrodes are well known to be critical components because their properties influence the capacitance of the supercapacitor. Carbon nanotubes (CNTs) seem to be one of the most promising solutions among the several different types of electrodes that have been investigated in the literature. This is because of their chemical and thermal stability as well as their high surface area and ideal percolated pore structure [5–10]. In particular, best electrochemical performance was proven for electrodes made with vertically aligned CNTs (VANTs) because of the high number of accessible pores of 2–5 nm in size [10–14]. The electrolytes voltage window is also critical because it influences the energy density and the power density (which are proportional to the voltage squared) of the overall device. Aqueous electrolytes are characterized by a narrow electrochemical window (1 V), instead the organic electrolytes have relatively larger windows (2–3 V) but suffer from serious health and safety problems as they are volatile, flammable and can be toxic. Room-temperature ionic liquid electrolytes (RTILs), which are molten salts with a melting point close to or below room temperature, have the potential to surpass the currently available aqueous and organic electrolytes. This is because they are composed of ions of opposite charges and are characterized by high conductivity, nonvolatility, low toxicity, large electrochemical window and good electrochemical stability. These characteristics make RTILs, already used as solvents in several applications [15–17], suitable for supercapacitors [18,19]. Recently RTILs were incorporated into polymer electrolytes to obtain highly conducting and electrochemically stable electrolytes for solids state supercapacitors [20]. Moreover, there have been several studies on CNT-based supercapacitors with RTIL as electrolyte [21–25]. These studies showed that the combination: CNTs electrodes/RTIL led to a higher capacitance than the combinations: activated carbon/RTIL [21] or CNTs/organic electrolyte [24]. The CNTs pores size in fact matches perfectly the RTIL's ions size. Despite this major compatibility between CNTs electrodes and RTIL, these traditional systems are still lacking in performance especially in terms of power density and mechanical flexibility making them unsuitable for the realization of the above described flexible, free-standing and pre-fabricated functional film. The principal limitation of CNTs electrodes/RTIL supercapacitors is that the simple stacking of the key components (electrodes, separator and electrolyte) generates multiple interfaces and undesired interfacial debonding during the in-service life which causes a significant increase of the overall electrical resistance. A potential solution to realize the pre-fabricated films can be envisioned through the recently developed all-integrated paper and textile electronic devices [26–30] that led to a number of research activities on papers, sponges, clothes and textile-based energy storage devices. These studies demonstrated that carbon nanotubes and cellulose are suitable for the realization of free-standing and flexible electrodes [31–36]. The primary advantage of cellulose is that of being usable as spacer while providing inherent flexibility, porosity and ease of integration with carbon nanotubes [33], giving rise to an inexpensive and biocompatible system. The use of cellulose for supercapacitors started being considered suitable in Refs. [37,38] where it was shown for the first time that cellulose could be dissolved in alkyl substituted imidazolium RTILs [39], and through numerous studies that were carried out on dissolution optimization and future applications [40–44]. Consequently, the first and only flexible and free-standing supercapacitor made of a monolithic layer of carbon nanotubes electrodes soaked in a solution of cellulose in RTIL, was soon demonstrated [38]. Despite this latter interesting attempt with a resulting capacitance of 22 F g^{-1} and energy density of 13 Wh Kg^{-1} comparable with those of paper-based CNTs supercapacitors [31,34], the device suffered a rather complex and costly fabrication process, high equivalent series resistance (ESR) and, therefore, low power density. These drawbacks were caused by the adopted chloride based RTIL which is viscous and solid at room temperature. These properties not only require a significant number of fabrication steps for the CNTs integration, but also, and most importantly, lead to low ions mobility [45,46] compared to acetate based RTILs which have low melting point and low viscosity [40,42,45]. Cellulose solution in acetate based RTIL was successfully included in commercially available MWNTs to produce conductive cable fibers with insulating surface [43] and, more recently, cellulose solution in acetate based RTIL was used for the first time for the realization of supercapacitors with activated carbon electrodes. The resulting devices were found to display high performance in terms of specific capacitance and cyclic stability [47,48].

In this paper a novel nanostructured, free-standing, monolithic and functional film (only a few hundred micrometers thick) based on VANTs integrated in a 5 w% solution of cellulose in 1-ethyl-3-methylimidazolium acetate (EMIM Ac) is presented for high-power, easy-to assemble and 3-D shape-adaptable supercapacitors. The design of the proposed pre-fabricated film is such to avoid undesired discontinuities to ions mobility. Consequently, energy losses are drastically reduced and an unprecedented rapid and low-cost fabrication procedure is guaranteed. Thus, this work solves the key limitations related to fabrication complexity and low power density of previously reported cellulose-based VANTs supercapacitors in RTIL [38].

2. Experimental

2.1. Design of the monolithic functional film

The design of the pre-fabricated, monolithic functional film is shown in Fig. 1. In this design, the two active electrodes that store ions are made of a high density array of vertically aligned carbon nanotubes (VANTs), as schematically represented in Fig. 1(b). The two electrodes, which face each other with a pre-defined inter-space distance, as required to avoid circuit-shortage, are embedded into a cellulose/RTIL (EMIM Ac) layer which constrains the electrodes into their fixed relative position while conferring a hosting matrix, ions and their full mobility. The electrode thickness (VANTs length) is defined by simultaneously taking into account, as discussed in Section 2.2, the ideal VANTs length that maximizes the electrochemical performance [49] in conjunction with specific manufacturing strategies for the realization of the free-standing and monolithic film. The result of the described assembly is a fully functional nanostructured film that can be used as easy-to-assemble supercapacitors by simply connecting it to current collectors. The film is additionally characterized by a certain degree of flexibility given by the integration of VANTs into this unique hosting matrix.

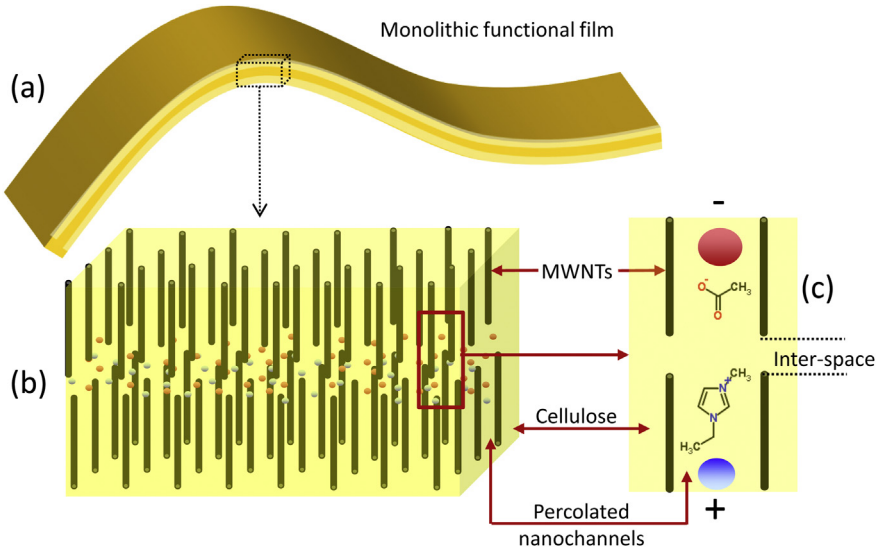

Fig. 1. (a) Schematic of the pre-fabricated monolithic functional film; (b) Higher magnification of the film in a polarized state highlighting the VANTs electrodes integrated with 5 wt % solution of cellulose in EMIM Ac with an inter-space between the electrodes. (c) Higher magnification showing the nanochannels percolated with the polarized RTIL electrolyte and the inter-space between the electrodes.

The mechanical flexibility allows the film to adapt to 2-D and/or 3-D shapes significantly expanding its usage to a wide range of applications.

2.2. Electrodes synthesis and strategic film fabrication

The strategic choice of the EMIM Ac electrolyte ("Cellionic BCW1100", Aldrich) leads to an extremely simple fabrication process which consists of the following two key steps: (1) the VANTs carpet growth to form the two electrodes and; (2) the infiltration into the carpets of the 5 wt % solution of cellulose in the electrolyte to form an uniform film of cellulose/electrolyte embedding the nanotubes. Within the first step, VANTs carpets were grown on a silicon piece with the procedure previously reported in Ref. [49] with the only addition of a 5 min annealing in Hydrogen at a flow rate of 300 sccm. This was done to obtain a distribution of catalyst nanoclusters such to allow the realization of densely packed carbon nanotubes. The VANTs deposition time was tuned at 20 min to obtain a carpet that was sufficiently thick to be suitable for the following fabrication step (electrode fabrication), but, at the same time, sufficiently thin to maximize the electrochemical performance that was reported to be strongly affected by the VANTs length [49].

A drop of cellulose solution in electrolyte was spin-coated for 5 min at 8000 rpm on the as-grown VANTs carpet (Fig. 2(a)). The duration of the spinning process was found to be critical to remove any residual drop of liquid from the carpet as required to make the film. Finally the MWNTs/electrolyte/cellulose film was easily removed from the silicon substrate using a blade (Fig. 2(b)). The success of the previous step requires that the carpet thickness is perfectly tuned with the amount of electrolyte. If the carpet thickness and the amount of electrolyte are not tuned, the MWNTs/cellulose/electrolyte film would in fact turn into a gel [46,50] and this not only would make the removal process (from silicon) a difficult step, but, most importantly, would have a detrimental effect on the film which would lose its ideal free-standing function. The electrode was then faced and monolithically bonded to another electrode by an additional layer of a cellulose/electrolyte solution which also helped in preventing electrical shortage (Fig. 2(c)). The image in Fig. 2(d) shows the flexibility of the pre-fabricated fully functional film which was bended repeatedly without creating breaks or debonds, visible by naked eye, as expected thanks to the monolithic nature of the film. This promising mechanical flexibility of the film is under investigation by means of ad-hoc experimental testing. It is worth noting that all the fabrication steps were performed at room

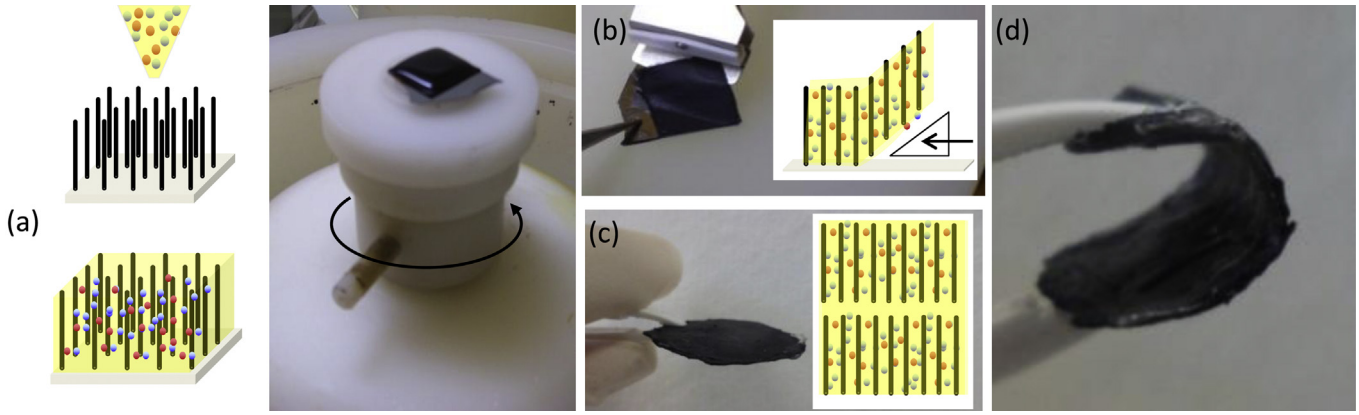

Fig. 2. (a)–(c) Fabrication of the monolithic and functional film: (a) spinning of cellulose solution on VANTs previously grown on Si substrate; (b) removal of the resulting electrode from Si; (c) overlapping of two inter-spaced electrodes. (d) Bending of the functional film to show its flexibility.

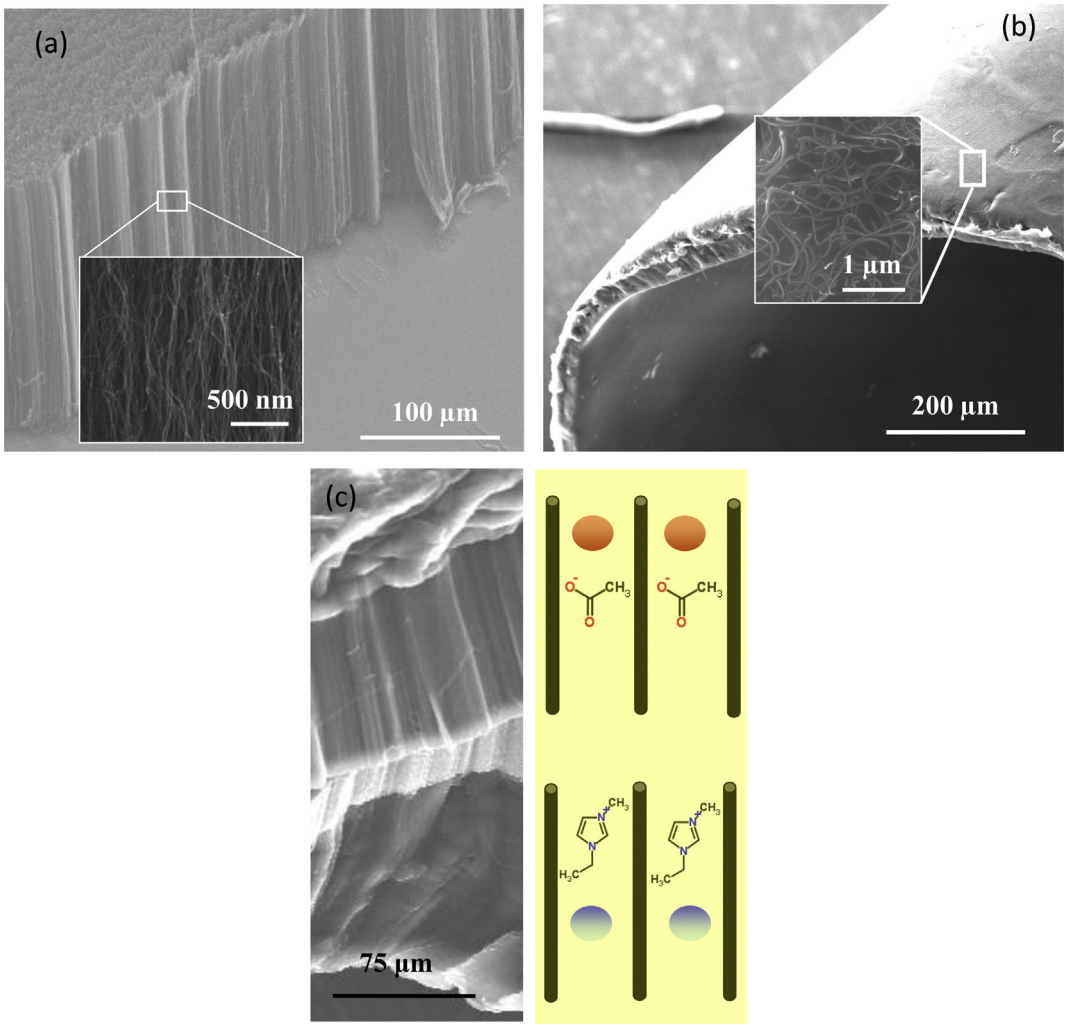

Fig. 3. SEM analysis: (a) VANTs on Si, the inset shows the alignment and the density at high magnification; (b) nanocomposite electrode in a bended state; the inset shows a higher magnification of the VANTs embedded in the cellulose/electrolyte solution; (c) cross-section of the monolithic functional film in a polarized state where each single layer is specified through the scheme on the right.

temperature thanks to the low melting point of the electrolyte (15 °C), therefore the whole procedure was extremely simple and fast.

2.3. Fabrication of the electrochemical test cells

The free-standing monolithic film of 15 mm in diameter was vacuum dried overnight at 80 °C to remove any residual air and moisture, that, if trapped in the electrodes, can degrade the electrolyte and (moisture) can interfere with the cellulose dissolved in EMIM Ac [51,52]. A coin-type test cell (El Cell) was prepared in a glove box under an argon environment and was used to analyze the electrochemical response of the fabricated nanostructured film that, once sandwiched within the gold current collectors of the cell, behaves as a supercapacitor. The electrical contact between the film and the collectors was guaranteed by applying a 25 N constant load through a spring.

2.4. Measurements and characterization

The novel nanostructured composite film was examined both by morphological analysis with a scanning electron microscope (SEM, Philips, ESEM XL 30) and by electrochemical measurements with a Versastat 4 Potentiostat/Galvanostat/FRA (Princeton Applied Research). Cyclic voltammetry (CV), galvanostatic charge/discharge (GC) and electrochemical impedance spectroscopy (EIS) measurements were performed to evaluate the capacitive behavior, the durability and the electrochemical parameters (specific electrode capacitance, knee frequency end equivalent series resistance (ESR)). The supercapacitor cell was tested in a two-electrode configuration in order to simulate the real electrochemical behavior and prevent the results overestimation [53].The CV tests were carried out at 1000 and 100 mV s^{-1}, impedance tests were carried out at: a dc bias of 0 V, a sinusoidal signal of 10 mV in amplitude, and a frequency range of 10 kHz to 10 mHz. The ESR and the knee frequency were deduced from the complex-plane impedance spectra. GC tests were performed with a current density that ranged from 1 to 30 A g^{-1}. To evaluate the cycle life of supercapacitor 2000 consecutive and complete galvanostatic charge–discharge cycles at 10.7 A g^{-1} current density were performed.

3. Results and discussion

SEM images of the grown VANTs carpets, on silicon and assembled to form the functional film are shown in Fig. 3. The VANTs are uniformly and vertically distributed with an average length (electrode thickness) of 160 µm (see Fig. 3(a)) as planned by tuning the fabrication process with the electrochemical properties.

(see the procedure specified in Section 2.2). The MWNTs in the carpet have an average external diameter of 7–10 nm and are densely packed with an average inter-tube distance of 50 nm (see inset in Fig. 3(a)). The SEM image in Fig. 3(b) shows a bended state of the electrode after removal from the silicon substrate as well as the nanoscopic nature of the cellulose/electrolyte solution (see inset in Fig. 3(b)). The nanotubes dipped in the cellulose solution don't show any form of entanglement and the solution is penetrated all over the nanotubes interspaces. This is indeed very important to guarantee the full exposure of the VANTs to the electrolyte, thus, to allow ions to reach and use the entire nanotubes length in order to maximize the functional performance once the film is used for supercapacitors applications [49]. The full penetration of the solution within the nanotubes is also important to guarantee the global flexibility and the monolithic and free-standing nature of the functional film. The VANTs carpets can in fact be viewed globally as a highly porous foam-like material made, locally, of discrete solid elements (the nanotubes) that are not physically interconnected, but interact within each other through weak electrostatic forces. This type of interaction confers to the porous material a discrete nature and a certain degree of flexibility given by the allowed relative motion between each single nanoscopic solid element. The cellulose solution that fills the interspaces to form the nanocomposite electrode, transforms the porous material into a continuous, monolithic and, indeed, still flexible material. Fig. 3(c) shows the cross-section of the fully assembled monolithic functional film (350 μm thick) which consists of two VANTs electrodes embedded in cellulose/EMIM Ac electrolyte and interspaced, at a pre-defined set distance of 35 μm, with cellulose dissolved in the electrolyte. The electrochemical response of the supercapacitor was evaluated by CV tests and GC tests (current density of 3.75 A g^{-1}). The capacitive response is nearly ideal as proven by the rectangular shape of the CV curves in Fig. 4(a) [11,54] and by the nearly triangular and symmetrical shape of the GC charge–discharges curves that also show a small IR drop that highlights the prominent capacitive behavior of the supercapacitor up to an operating voltage of 2 V (Fig. 4(b)).

The excellent electrical conductivity and mesoporosity of the CNTs/cellulose nanocomposite, perfectly tuned with the chosen electrolyte and electrode thickness (accordingly to Ref. [49]) to allow ions accessibility, could be responsible for the observed good capacitive response. The specific capacitance, *Cp*, of the nanocomposite electrode is calculated from the CV and GC curves using the following Eq. (1) and Eq. (2), respectively:

$$Cp\,(F \times g^{-1}) = q/\Delta V = \frac{\int_{Vi}^{Vf} i(V)\mathrm{d}V}{\Delta V \nu m} \tag{1}$$

$$Cp\left(F \times g^{-1}\right) = \frac{I}{\nu \times m} \times 2 \tag{2}$$

where $\nu(V\,s^{-1})$ is the scan rate applied in the CV measurements or the slope of the discharge curve after the *IR* drop in the GC test, *m* (*g*) is the mass of the single electrode, ΔV (*V*) is the voltage range between *Vi* and *Vf*, *i*(*V*) is the current response and *I*(*A*) is the constant discharge current of the GC measurements. The calculated capacitance are 34 F g^{-1} and 39 F g^{-1} for the CV (at 100 m V^{-1}) and the GC curves (at 3.57 A g^{-1}), respectively. These values are significantly higher than those reported in the literature for supercapacitors based on paper/CNTs nanocomposites [31,38] and for MWNTs-based supercapacitors with RTIL and organic electrolytes [14,23,25,55,56]. The charging/discharging rate capability of the supercapacitor, was evaluated performing charge/discharge tests with current densities that varied from 1 to 30 A g^{-1}which are much higher than those reported in the literature for similar systems. It is found that the capacitance of the cell decreases with increasing current density (see Fig. 5(a)), as also observed for carbon/paper-based supercapacitors [31,34], because the electrode surface area accessible to ions decreases correspondingly. The cycle life of the electrode was evaluated under severe conditions by testing the supercapacitor for 2000 consecutive and complete galvanostatic charge–discharge cycles performed at 10.7 A g^{-1} current density while imposing the following voltage variation: 0 V, 2 V, 0 V. It is worth noting that this type of test analyzes the performance of the electrochemical devices under more severe conditions than typical lifetime studies which are performed at half-depth discharge (see Fig. 5(b)).

However, despite this unfavorable test, the nanostructured composite film exhibits an almost stable electrochemical response (starting from 500 cycles) reaching a total decline (after 2000 cycles) of 12.96%. This result is probably caused by a slight debonding between the CNTs and cellulose [57]. The initial capacitance reduction can be considered acceptable in view of the above mentioned severe tests in terms of current density and voltage window. The stable electrochemical response, highlighted by the resulting long cyclic stability, suggests that the novel nanostructured film is suitable for applications that require reliable energy storage devices over an extended lifetime. The ideal

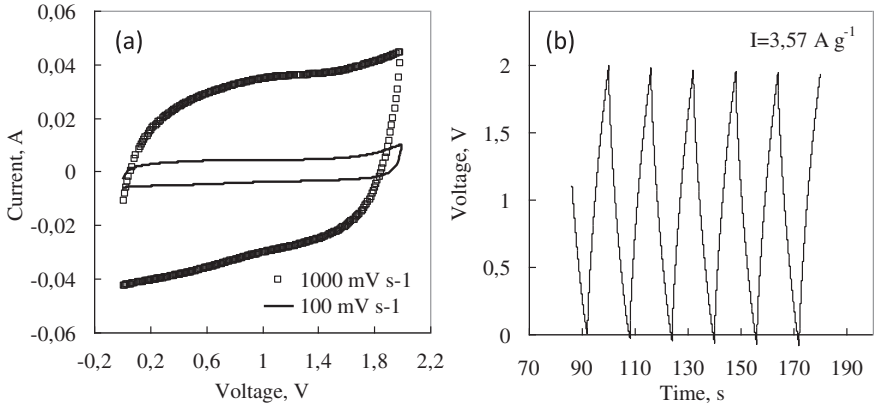

Fig. 4. Electrochemical response of a supercapacitor made with the monolithic functional film: (a) CV curves at a scan rate of 1000 and 100 mV s^{-1}; (b) GC curves at 3.75 A g^{-1} current density.

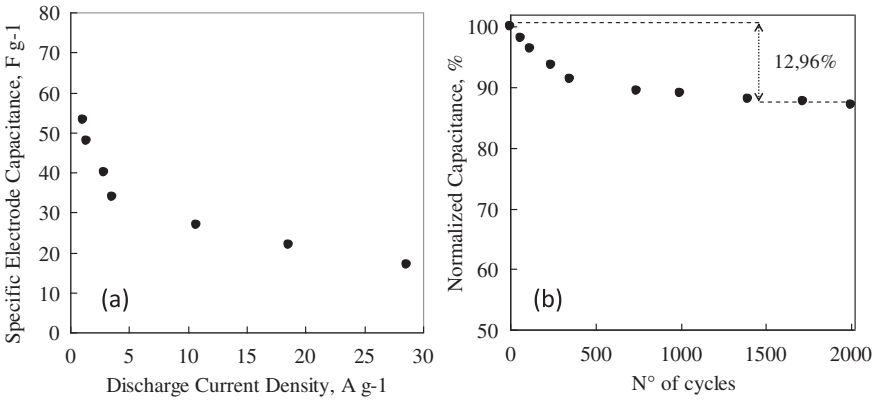

Fig. 5. Electrochemical response of supercapacitors made with the functional film: (a) Specific capacitance vs current density plot. (b) Normalized capacitance up to 2000 charge/discharge cycles at the current density of 10.7 A g^{-1}.

capacitive behavior of the supercapacitor is again highlighted by the complex-plane impedance plot in Fig. 6. The nearly vertical trend in the low frequency region proves that ions in the electrolyte diffuse easily inside the pore structure of the VANTs/cellulose and this process is not inhibited by the cellulose within the nanotubes. The equivalent series resistance (ESR) of the supercapacitor, determined from the intercept of the curve with the real axis, is 0.66 Ω (see inset Fig. 6). This ESR value is extremely lower than CNTs-solid state supercapacitors reported in literature [35,36,58] and MWNTs-based supercapacitors with RTIL and organic electrolyte [24,55,56]. The analysis of the graph in the high frequency region highlights a good electrical contact between the electrodes and the current collector (there are no semicircles in that areas). Finally, the analysis of the 45° Warburg region shows the low resistance to ions penetration in the electrode-electrolyte interface (the interface between the nanotubes surface and the electrolyte) and along the thickness of the porous electrode structure. Fig. 6 also shows that the knee frequency (critical frequency where a supercapacitor begins to exhibit the capacitive behavior) which is 19.9 Hz, is higher than that of CNTs-solid state supercapacitors reported in literature [36] and MWNTs-based supercapacitors with non-aqueous electrolyte [14,21]. It is believed that the low ESR, the low resistance to ions penetration at the interface and along the electrode's thickness and the high knee frequency, can be related to the high ionic conductivity of the chosen electrolyte, to the absence of stacked layers within the film thickness and to the physical nature of the matrix that hosts the VANTs. This matrix is substantially a viscous solution of cellulose dissolved in the electrolyte which clearly allows for a higher ions mobility than in solid-state as well as in any supercapacitor in which ions must find their path through a solid material. The maximum specific power density $P_{\text{cell max}}$, which is 108.23 kW kg^{-1}, is calculated using the following equation:

$$P_{\text{cell max}}\left(\text{KW}\times\text{Kg}^{-1}\right)=\frac{1}{4}\times\frac{Vf^2}{\text{ESR}\times m_{\text{tot}}} \tag{3}$$

where V_f (V) is the voltage at the end of charge, m_{tot} is the mass of the two electrodes (g). This value is higher than CNTs/paper or polymer composite supercapacitors reported in literature [21,34–36,58]. Fig. 7(a) shows the Ragone plot that summarizes the energy and power density at different discharge current densities. The energy density of the supercapacitor $W_{\text{cel lsp}}$ is calculated with the following equation:

$$W_{\text{cell sp}}\left(\text{Wh}\times\text{Kg}^{-1}\right)=\frac{1}{2}\times\frac{C\times V^2}{3.6\times m_{\text{tot}}} \tag{4}$$

where C is the capacitance (F) calculated from the charge discharge curves at different discharge current densities, V is the voltage range (2 V for our tests), 3.6 is the conversion factor to obtain the specific energy density in Wh × Kg^{-1} and, m_{tot} (g) is the total mass of both electrodes. The power density of the supercapacitor ($P_{\text{cell sp}}$) is calculated with the following equation:

$$P_{\text{cell sp}}\left(\text{KW}\times\text{Kg}^{-1}\right)=\frac{W_{\text{sp}}}{\Delta t} \tag{5}$$

where Δt is the discharge time corresponding at each discharge current density. The maximum calculated value of energy density, within the analyzed current density range, is 14.72 Wh Kg^{-1} at 1 A g^{-1} which is higher than other cellulose-based supercapacitors reported in literature [38] while the minimum value is 4.72 Wh Kg^{-1} at 28.57 A g^{-1}. The calculated power density reaches a maximum of 36.17 kW kg^{-1} at 28.57 A g^{-1} and a minimum of 0.53 kW kg^{-1} at 1 A g^{-1}. At an intermediate value of 10.7 A g^{-1} current density, the energy and power density set at a calculated value of 7.5 Wh Kg^{-1} and 13.5 kW kg^{-1} respectively and, accordingly to Fig. 5(b), were then found to decrease reaching respectively, after 2000 cycles a value of 6.53 Wh Kg^{-1} and 11.75 kW kg^{-1} Fig. 7(b) shows the comparison of various CNT supercapacitors in terms of electrochemical performance. The energy density values

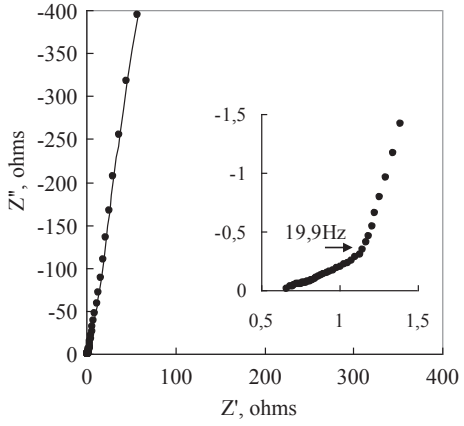

Fig. 6. EIS plot: the inset shows the high frequency region highlighting the knee frequency.

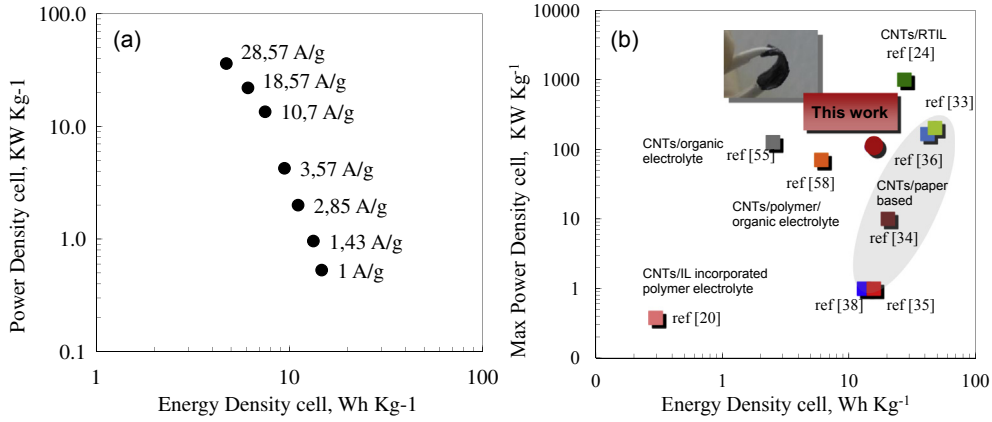

Fig. 7. Performance of a supercapacitor made with the monolithic functional film: (a) Ragone plot with the used current densities; (b) Comparison of a supercapacitor made with the proposed functional film with various non aqueous and/or polymer and paper based system.

that are inserted in the plot, represent the maximum values of the GC tests reported in the literature, while the maximum power density values are calculated with Eq. (3). Similarly, the values of our device (energy density of 14.72 Wh Kg^{-1} at 1 A g^{-1} and maximum power density of 108.23 kW kg^{-1}) that have been inserted in the plot for comparison with the devices in the literature, were calculated using the GC test and Eq. (3) for maximum power density, where ESR is 0.66 Ω and is determined from the intercept of the complex-plane impedance plot with the real axis. Moreover for further information, the ESR is also often calculated from the IR drops [53] and depends on the current density. Thus, ESR calculated at the highest current density used, 28.57 Ag^{-1}, is 0.875 Ω from the following equation

$$\mathrm{ESR} = \Delta V/(2xI) \tag{6}$$

where ΔV is the IR drop of the GC curve and I is 28.57 Ag^{-1} and the maximum power density calculated is therefore 81.63 KW Kg^{-1}. This comparison clearly highlights that the novel nanostructured film proposed by the authors is superior in its performance than the most important and representative systems that were proposed with carbon nanotubes and organic or ionic liquid electrolyte using either polymer or paper binders (see Refs. [34], [35], [58], [20], [38]). Just a few cellulose-based systems reported in the literature, see Refs. [33], [36], show a superior performance in terms of both energy and power density mainly thanks to the adopted type of nanotubes (single [33] or double-walled [36]).

4. Conclusions

In this work, a novel monolithic and pre-fabricated fully functional film was proposed for high energy, high power density, flexible supercapacitors. The materials involved (VANTs, EMIM Ac and cellulose) allowed, after an accurate matching process between the nanotubes length and the amount of electrolyte/cellulose solution, to obtain a nanostructured film which functions simultaneously as electrode, electrolyte and separator without physical discontinuity. The presented film can be used for a wide range of applications that require light-weight, flexible energy storage devices. The nanostructured film is characterized by excellent electrochemical properties and long cycle life. The low ESR, 0.66 Ω, and high knee frequency (19.9 Hz), lead to a supercapacitor with high maximum power density P_{max} (108.23 kW kg^{-1}) and with a reaction speed that is suitable for fast charging/discharging events. The performance (in terms of energy and power density) of the proposed nanostructured film, used as a supercapacitor, places it among the best non-aqueous electrolyte systems presented thus far in the literature.

Acknowledgments

The research leading to these results was supported by the Specialized International Collaborative Program (Grant No. UD090080GD) under the Agency for Defense Development (ADD), Republic of Korea and by the European Research Council under the European Union's Seventh Framework Programme (FP/2007-2013)/ ERC Grant Agreement n. 308261 and by the Italian Ministry of Education and Research under the Rita Levi Montalcini Program.

References

[1] P. Lua, D. Xuea, H. Yangc, Y. Liuc, Int. J. Smart Nano Mater. (2012) 1–25. First.
[2] J.R. Miller, P. Simon, Science 321 (2008) 651–652.
[3] Y. Sun, J.A. Rogers, Adv. Mater. 19 (2007) 1897–1916.
[4] D.H. Kim, J.H. Ahn, W.M. Choi, H.S. Kim, T.H. Kim, J.Z. Song, Y.G.Y. Huang, Z.J. Liu, C. Lu, J.A. Rogers, Science 320 (2008) 507–511.
[5] E. Frackowiak, K. Jurewicz, S. Delpeux, F. Béguin, J. Power Sources 97–98 (2001) 822–825.
[6] E. Frackowiak, F. Béguin, Carbon 39 (6) (2001) 937–950.
[7] E. Frackowiak, K. Metenier, V. Bertagna, F. Béguin, Appl. Phys. Lett. 77 (2000) 2421–2423.
[8] M. Inagaki, H. Konno, O. Tanaike, J. Power Sources 195 (24) (2010) 7880–7903.
[9] K.H. An, W.S. Kim, Y.S. Park, Y.C. Choi, S.M. Lee, D.C. Chung, D.J. Bae, S.C. Lim, Y.H. Lee, Adv. Mater. 13 (7) (2001) 497–500.
[10] P. Simon, Y. Gogotsi, Nat. Mater. 7 (2008) 845–854.
[11] C. Du, J. Yeh, N. Pan, Nanotechnology 16 (2005) 350–353.
[12] D. Zilli, P.R. Bonelli, A.L. Cukierman, Nanotechnology 17 (2006) 5136–5141.
[13] H. Zhang, G. Cao, Y. Yang, Energy Environ. Sci. 2 (2009) 932–943.
[14] H. Zhang, G. Cao, Y. Yang, J. Power Sources 172 (2007) 476–480.
[15] T. Welton, Chem. Rev. 99 (8) (1999) 2071–2084.
[16] M.J. Earle, K.R. Seddon, Pure Appl. Chem. 72 (7) (2000) 1391–1398.
[17] P. Wasserscheid, W. Keim, Angew. Chem. Int. Ed. Engl. 39 (21) (2000) 3772–3789.
[18] A. Lewandowski, M. Galinski, J. Phys. Chem. Solids 65 (2004) 281–286.
[19] D.R. Macfarlane, M. Forsyth, P.C. Howlett, J.M. Pringle, J. Sun, G. Annat, W. Neil, E.I. Izgorodina, Acc. Chem. Res. 40 (2007) 1165–1173.
[20] G.P. Pandey, Y. Kumar, S.A. Hashmi, Solid State Ionics 190 (2011) 93–98.
[21] W. Lua, L. Qub, K. Henrya, L. Dai, J. Power Sources 189 (2009) 1270–1277.
[22] J.N. Barisci, G.G. Wallace, D.R. MacFarlane, R.H. Baughman, Electrochem. Commun. 6 (2004) 22–27.
[23] W. Lu, R. Hartman, J. Phys. Chem. Lett. 2 (2011) 655–660.
[24] B. Kim, H. Chung, W. Kim, Nanotechnology 23 (2012) 155401.
[25] B. Xu, F. Wu, R. Chen, G. Cao, S. Chen, G. Wang, Y. Yang, J. Power Sources 158 (2006) 773–778.
[26] P. Andersson, D. Nilsson, P.O. Svensson, M.X. Chen, A. Malmstrom, T. Remonen, T. Kugler, M. Berggren, Adv. Mater. 14 (2002) 1460–1464.
[27] F. Eder, H. Klauk, M. Halik, U. Zschieschang, G. Schmid, C. Dehm, Appl. Phys. Lett. 84 (2004) 2673–2675.

[28] D.H. Kim, Y.S. Kim, J. Wu, Z.J. Liu, J.Z. Song, H.S. Kim, Y.G.Y. Huang, K.C. Hwang, J.A. Rogers, Adv. Mater. 21 (2009) 3703–3707.
[29] B. Lamprecht, R. Thünauer, M. Ostermann, G. Jakopic, G. Leising, Phys. Status Solidi A 202 (2005) R50–R52.
[30] N.W.C. Kaihovirta, T. Makela, C. Wilen, R. Osterbacka, Adv. Mater. 21 (2009) 2520–2523.
[31] L. Hu, H. Wu, Y. Cui, Appl. Phys. Lett. 96 (2010) 183502.
[32] L. Hu, H. Wu, F. La Mantia, Y. Yang, Y. Cui, ACS Nano 4 (10) (2010) 5843–5848.
[33] L. Hua, J.W. Choi, Y. Yang, S. Jeong, F. La Mantia, L.F. Cui, Y. Cui, PNAS 106 (51) (2009) 21490–21494.
[34] L. Hu, M. Pasta, F. La Mantia, L.F. Cui, S. Jeong, H.D. Deshazer, J.W. Choi, S.M. Han, Y. Cui, Nano Lett. 10 (2) (2010) 708–714.
[35] Y.J. Kang, S.J. Chun, S.S. Lee, B.Y. Kim, J.H. Kim, H. Chung, S.Y. Lee, W. Kim, ACS Nano 6 (7) (2012) 6400–6406.
[36] Y.J. Kang, H. Chung, C.H. Han, W. Kim, Nanotechnology 23 (2012) 065401.
[37] D. Wei, S.J. Wakeham, T.W. Ng, M.J. Thwaites, H. Brown, P. Beecher, Electrochem. Commun. 11 (12) (2009) 2285–2287.
[38] V.L. Pushparaj, M.M. Shaijumon, A. Kumar, S. Murugesan, L. Ci, R. Vajtai, R.J. Linhardt, O. Nalamasu, P.M. Ajayan, PNAS 104 (34) (2007) 13574–13577.
[39] R.P. Swatloski, S.K. Spear, J.D. Holbrey, R.D. Rogers, J. Am. Chem. Soc. 124 (2002) 4974–4975.
[40] M. Gericke, P. Fardim, T. Heinze, Molecule 17 (2012) 7458–7502.
[41] L. Meli, J. Miao, J.S. Dordick, R.J. Linhardt, Green. Chem. 12 (2010) 1883–1892.
[42] Y. Cao, J. Wu, J. Zhang, H. Li, Y. Zhang, J. He, Chem. Eng. J. 147 (2009) 13–21.
[43] M. Miyauchi, J. Miao, T.J. Simmons, J.W. Lee, T.V. Doherty, J.S. Dordick, R.J. Linhardt, Biomacromolecules 11 (2010) 2440–2445.
[44] J. Vitz, T. Erdmenger, C. Haensch, U.S. Schubert, Green. Chem. 11 (2009) 417–424.
[45] S. Fendt, S. Padmanabhan, H.W. Blanch, J.M. Prausnitz, J. Chem. Eng. Data 56 (2011) 31–34.
[46] F. Endres, S.Z. El Abedinw, Phys. Chem. 8 (2006) 2101–2116.
[47] A. Brandt, S. Pohlmann, A. Varzi, A. Balducci, S. Passerini, MRS Bull. 38 (2013) 554–559.
[48] N. Böckenfeld, S.S. Jeong, M. Winter, S. Passerini, A. Balducci, J. Power Sources 221 (2013) 14–20.
[49] L. Basiricò, G. Lanzara, Nanotechnology 23 (30) (2012) 305401.
[50] T. Fukushima, A. Kosaka, Y. Ishimura, T. Yamamoto, T. Takigawa, N. Ishii, T. Aida, Science 300 (2003) 2072–2074.
[51] K.A. Le, R. Sescousse, T. Budtova, Cellulose 19 (2012) 45–54.
[52] O. Kuzmina, E. Sashina, D. Wawro, S. Troshenkowa, Fibres Text. East. Eur. 18 (3(80)) (2010) 32–37.
[53] M.D. Stoller, R.S. Ruoff, Energy Environ. Sci. 3 (2010) 1294–1301.
[54] B.E. Conway, Electrochemical Supercapacitor: Scientific Fundamentals and Technological Application, Kluwer Academic/Plenum Publisher, New York, 1999.
[55] Y. Honda, T. Haramoto, M. Takeshige, H. Shiozaki, T. Kitamura, M. Ishikawa, Electrochem. Solid-State Lett. 10 (4) (2007) A106–A110.
[56] B. Kim, H. Chung, B.K. Min, H. Kim, W. Kim, Bull. Korean Chem. Soc. 31 (12) (2010) 3697–3702.
[57] G. Formica, W. Lacarbonara, Compos. Struct. 96 (2013) 514–525.
[58] M. Kaempgen, C.K. Chan, J. Ma, Y. Cui, G. Gruner, Nano Lett. 9 (5) (2009) 1872–1876.